J. Fluid Mech. (1983), *vol.* 132, *pp.* 49–63
Printed in Great Britain

Thermal instability of two-dimensional stagnation-point boundary layers

By K. CHEN†, M. M. CHEN AND C. W. SOHN‡
Department of Mechanical and Industrial Engineering, University of Illinois, Urbana, Illinois 61801

(Received 13 August 1982 and in revised form 15 February 1983)

A study of thermal instability for the two-dimensional stagnation flow for Prandtl numbers ranging from 0.7 to infinity is presented. The analysis represents an exact solution since neither the boundary-layer approximation nor the parallel-flow assumption was invoked. Of particular interest is that the critical Rayleigh number and the critical wavenumber, when defined on the basis of the thermal boundary-layer lengthscale, are found to be relatively insensitive to the Prandtl number for the range of Prandtl numbers studied.

1. Introduction

When a rising hot plume impinges on a cold boundary, or when a descending cold jet impinges on a warm boundary, a stagnation boundary layer is formed which may become gravitationally unstable. The problem can be viewed as the prototype of thermal-instability problems for forced convection boundary layers. This is because the stagnation boundary layer, having a uniform thickness, possesses mathematical properties that render an exact analysis possible. In contrast, the study of boundary layers with variable thicknesses generally must invoke some form of parallel-flow assumption (Sparrow & Husar 1969; Lloyd & Sparrow 1970; Cheng & Wu 1976; Chen & Mucoglu 1979). A study of the thermal-instability problem for the stagnation boundary layer will thus provide an interesting basis of comparison for similar problems for all boundary layers. The problem is also a component of a model of high-Rayleigh-number convection above a heated surface previously proposed by one of the authors (Chen 1971).

Previous studies on thermal instability of shear flows (e.g. Chandra 1938; Ingersoll 1966) have consistently shown that the least-stable mode for moderate-to-large Prandtl numbers consists of non-oscillatory rolls with axes parallel to the direction of flow at the surface. The study of oscillatory modes will thus not be taken up in this communication. For two-dimensional stagnation boundary layers, these rolls are parallel to each other and of constant height and width, permitting the reduction of the instability problem to a one-dimensional eigenvalue problem without further simplifying assumptions, as will be shown later. For axisymmetric stagnation boundary layers, the streamwise rolls correspond to cells whose widths increase radially. Consequently, exact solutions will no longer be possible. At large distances

† Present address: Department of Mechanical and Industrial Engineering, University of Utah, Salt Lake City, Utah 84112.
‡ Present address: Construction Engineering Research Laboratory, U.S. Army Corps of Engineers, Champaign, Illinois 61820.

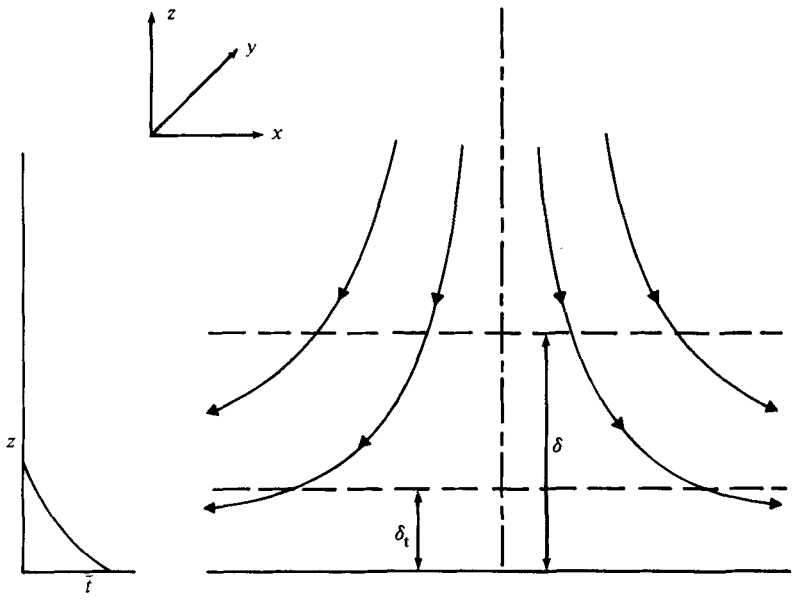

FIGURE 1. The model. Also shown are the temperature distribution and the coordinate system. Note that the figure shows a warm surface under a cool fluid, in conformity with common practice in thermal-stability studies. The figure would be inverted if the problem is viewed as the impingement of a warm plume on a cool ceiling.

from the centre, however, the behaviour of the axisymmetric stagnation flow is expected to approach the two-dimensional stagnation flow.

2. Formulation

The coordinate system employed is shown in figure 1. Note that z is the vertical coordinate measured from the surface and x and y are in the streamwise and spanwise directions respectively.

The intrinsic length and velocity scales for viscous stagnation flow are $(\nu/a)^{\frac{1}{2}}$ and $(\nu a)^{\frac{1}{2}}$ respectively, where ν is the kinematic viscosity and a is the free-stream velocity gradient $\partial u_\infty/\partial x$. Introducing the set of scales $(\nu/a)^{\frac{1}{2}}$, $(\nu a)^{\frac{1}{2}}$, $t_w - t_\infty$, $\rho\nu a$, $1/a$ for length, velocity, temperature, pressure and time, the non-dimensional governing equations, based on the assumption of linear equation of state and Boussinesq approximation, are

$$\nabla \cdot \boldsymbol{u}^* = 0, \tag{1}$$

$$(\partial \boldsymbol{u}^*/\partial \tau^*) + \boldsymbol{u}^* \cdot \nabla \boldsymbol{u}^* = -\nabla p^* + \nabla^2 \boldsymbol{u}^* + Gr^* \boldsymbol{k} t^*, \tag{2}$$

$$\frac{\partial t^*}{\partial \tau^*} + \boldsymbol{u}^* \cdot \nabla t^* = \frac{1}{Pr} \nabla^2 t^*, \tag{3}$$

where the velocity $\boldsymbol{u} = (u, v, w)$, p is the pressure, t_w and t_∞ the wall temperature and the free-stream temperature respectively, τ the time, ρ a constant density and $\boldsymbol{k}$ the unit vector in the positive z-direction. The two parameters appearing in these equations are the Prandtl number

$$Pr = \frac{\nu}{\alpha} \tag{4}$$

and the Grashof number defined with respect to the length $(\nu/a)^{\frac{1}{2}}$,

$$Gr^* = \left[\beta \Delta t\, g \left(\frac{\nu}{a}\right)^{\frac{3}{2}}\right] \Big/ \nu^2, \tag{5}$$

where g is the gravitational acceleration, α and β are the thermal diffusivity and coefficient of thermal expansion of the fluid, and Δt is the difference between t_w and t_∞.

The asterisk indicates that these dimensionless quantities are defined on the basis of the viscous scale and should be distinguished from the thermal scale to be discussed later. Note also that we have chosen a Grashof-number normalization instead of the more familiar Rayleigh-number normalization. This is done because Gr^* based on the length $(\nu/a)^{\frac{1}{2}}$ coincides with the Rayleigh number based on the thermal boundary-layer scale, to be discussed later, and is thus a more suitable indication of stability. The base flow of the instability problem is the classical Hiemenz flow

$$\bar{u}^* = x^* \phi'(z^*), \tag{6}$$

$$\bar{v}^* = 0, \tag{7}$$

$$\bar{w}^* = -\phi(z^*), \tag{8}$$

$$\bar{t}^* = \theta(z^*), \tag{9}$$

where ϕ and θ are solutions of the systems

$$\phi''' + \phi\phi'' - \phi'^2 = -1, \tag{10}$$

$$\phi(0) = \phi'(0) = 0, \quad \phi'(\infty) = 1, \tag{11}$$

$$-\phi\theta' = \frac{1}{Pr}\theta'', \tag{12}$$

$$\theta(0) = 1, \quad \theta(\infty) = 0, \tag{13}$$

Solutions for (10)–(13) are widely tabulated or can be easily generated by computation as is the case here.

For small disturbances, the disturbed flow is characterized by

$$u^* = x^* \phi' + \tilde{u}^*, \tag{14}$$

$$v^* = \tilde{v}^*, \tag{15}$$

$$w^* = -\phi + \tilde{w}^*, \tag{16}$$

$$p^* = \bar{p}^* + \tilde{p}^*, \tag{17}$$

$$t^* = \bar{t}^* + \tilde{t}^*. \tag{18}$$

Furthermore, we shall assume non-oscillatory parallel modes as discussed above:

$$(\tilde{u}^*, \tilde{v}^*, \tilde{w}^*, \tilde{p}^*, \tilde{t}^*) = (x^* U, V, W, P, T) e^{\sigma^* \tau^* + ik^* y^*}, \tag{19}$$

where U, V, W, P and T are functions of z^*. Note that the amplitude of $\tilde{u}^*$ depends linearly on x^* as in the case of $\bar{u}^*$. The appropriateness of this form can be verified

by substitution into (1)–(3). After linearization and setting $\sigma^* = 0$, the following set of equations for the amplitude functions is obtained:

$$U + ik^* V + W' = 0, \tag{20}$$

$$2U\phi' - \phi U' + W\phi'' = -k^{*2}U + U'', \tag{21}$$

$$-\phi V' = -ik^* P - k^{*2}V + V'', \tag{22}$$

$$-\phi W' - \phi' W = -P' + W'' - k^{*2}W + Gr^* T, \tag{23}$$

$$-\phi T' + W\theta' = \frac{-k^{*2}T + T''}{Pr}. \tag{24}$$

Eliminating V and P from the above equations results in three real equations for U, W and T:

$$U'' + \phi U' - (2\phi' + k^{*2})\, U - \phi'' W = 0, \tag{25}$$

$$W'''' + \phi W''' + (\phi' - 2k^{*2})\, W'' - k^{*2}\phi W' + (k^{*4} - k^{*2}\phi')\, W + U''' + \phi U'' + (\phi' - k^{*2})\, U' - k^{*2} Gr^* T = 0, \tag{26}$$

$$T'' + Pr\,\phi T' - k^{*2}T - Pr\,\theta' W = 0. \tag{27}$$

The boundary conditions are

$$U = W = W' = T = 0 \quad (z^* = 0, \infty). \tag{28}$$

3. Equations in stretched coordinates for large Pr

The only source of instability in the present problem is the buoyancy force existing near the wall. It decays very rapidly beyond the thermal boundary layer. Based on this fact, a normalization based on a thermal boundary-layer scale length rather than the viscous scale $(\nu/a)^{\frac{1}{2}}$ should be more appropriate, especially for large Pr. Since it is well known that as Pr increases, the ratio of the thermal boundary-layer thickness to the viscous boundary-layer thickness approaches $Pr^{-\frac{1}{3}}$, such a thermal scale is $(\nu/a)^{\frac{1}{2}} Pr^{-\frac{1}{3}}$ with the corresponding velocity scale $(\alpha a)^{\frac{1}{2}} Pr^{-\frac{1}{6}}$. We may thus define stretched variables, denoted by the superscript 0, as follows:

$$(\boldsymbol{r}^0; x^0, y^0, z^0) = (\boldsymbol{r}; x, y, z)\left(\frac{\nu}{a}\right)^{-\frac{1}{2}} Pr^{\frac{1}{3}}, \tag{29}$$

$$(\boldsymbol{u}^0; u^0, v^0, w^0) = (\boldsymbol{u}; u, v, w)\,(\alpha a)^{-\frac{1}{2}} Pr^{\frac{1}{6}}, \tag{30}$$

$$t^0 = \frac{t - t_\infty}{\Delta t}. \tag{31}$$

The velocity and the temperature can be separated into the base-flow solution and the perturbation solution as before. The equations governing the 'stretched' base-flow velocity function $\phi^0(z^0)$ and the temperature function $\theta^0(z^0)$ are

$$\frac{\phi^{0\prime 2}}{Pr} - \frac{\phi^0 \phi^{0\prime\prime}}{Pr} - \phi^{0\prime\prime\prime} = Pr^{-\frac{1}{3}}, \tag{32}$$

$$-\phi^0 \theta^{0\prime} = \theta^{0\prime\prime}, \tag{33}$$

where

$$\phi^0 = Pr^{\frac{2}{3}}\phi, \tag{34}$$

$$\theta^0 = \theta. \tag{35}$$

The counterpart of (19) is

$$(\tilde{u}^0, \tilde{v}^0, \tilde{w}^0, \tilde{p}^0, \tilde{t}^0) = (x^0 U^0, V^0, W^0, P^0, T^0) \exp(\sigma^0 \tau^0 + \mathrm{i} k^0 y^0), \tag{36}$$

where

$$k^0 = k^* Pr^{-\frac{1}{3}}. \tag{37}$$

The counterparts of (25)–(27) are

$$U^{0\prime\prime} + \frac{\phi^0 U^{0\prime}}{Pr} - \left(k^{02} + \frac{2\phi^{0\prime}}{Pr}\right) U^0 - \frac{W^0 \phi^{0\prime\prime}}{Pr} = 0, \tag{38}$$

$$W^{0\prime\prime\prime\prime} + \frac{\phi^0 W^{0\prime\prime\prime}}{Pr} + \left[\frac{\phi^{0\prime}}{Pr} - 2k^{02}\right] W^{0\prime\prime} - \left[\frac{k^{02}}{Pr}\phi^0\right] W^{0\prime} + \left[k^{04} - \frac{\phi^{0\prime} k^{02}}{Pr}\right] W^0$$
$$+ U^{0\prime\prime\prime} + \frac{\phi^0}{Pr} U^{0\prime\prime} + \left[\frac{\phi^{0\prime}}{Pr} - k^{02}\right] U^{0\prime} - k^{02} Ra^0 T^0 = 0, \tag{39}$$

$$T^{0\prime\prime} + \phi^0 T^{0\prime} - k^{02} T^0 - W^0 \theta^{0\prime} = 0. \tag{40}$$

The boundary conditions are

$$U^0 = T^0 = W^0 = W^{0\prime} = 0 \quad (z^0 = 0, \infty). \tag{41}$$

In the above, the Rayleigh number Ra^0 is based on the thermal boundary-layer lengthscale $(\nu/a)^{\frac{1}{2}} Pr^{-\frac{1}{3}}$:

$$Ra^0 \equiv g\beta\Delta t \left[\left(\frac{\nu}{a}\right)^{\frac{1}{2}} Pr^{-\frac{1}{3}}\right]^3 \Big/ \nu\alpha. \tag{42}$$

After simplification, it is seen that

$$Ra^0 \equiv Gr^*. \tag{43}$$

In other words, the Rayleigh number based on the thermal scale length is equal to the Grashof-number based on the viscous scale length. This explains the use of the Grashof-number normalization for (1)–(3).

Equations (38)–(41) are completely equivalent to (25)–(28). The principle advantage is that since the lengthscale used is more relevant to the thermal boundary layer, one may expect the critical Rayleigh number and the critical wavenumber based on the thermal scale $(\nu/a)^{\frac{1}{2}} Pr^{-\frac{1}{3}}$ to reach a finite limit as $Pr \to \infty$. No such limits exist for the critical Rayleigh number and the critical wavenumber defined on the basis of the viscous scale $(\nu/a)^{\frac{1}{2}}$.

4. The asymptotic behaviour of the disturbances far from the boundary

In the study of the stability of fluid layers bounded on one side only, the behaviour of the disturbances at large distances from the boundary is of considerable interest. Knowledge about the rate of decay of the disturbances is useful in assessing whether or not they are bounded in a given sublayer. Otherwise, this semi-infinite fluid layer may be unconditionally unstable. Furthermore, this knowledge is useful during numerical computation in selecting the size of the computed domain.

All variable coefficients in Equations (38) through (40) are multiples of the wavenumber k^0 and the base-flow solutions θ^0 and ϕ^0 and their derivatives. At large z^0, these either become constants or vary as z^0 or z^{02}. They are, therefore, relatively slowly varying functions. On the other hand, at large z^0, the disturbance functions tend to vary rather rapidly, as will be shown later. Hence, as a first approximation, $\theta^{0\prime}$ and $\phi^{0\prime\prime}$ can be neglected and the other coefficients assumed constant at large z^0.

This results in a homogeneous set of equations which has four exponentially growing and four exponentially decaying solutions:

$$W^0 = C_1 \exp(\alpha_1 z^0) + C_2 \exp(\alpha_2 z^0) + C_3 \exp(\beta_1 z^0) + C_4 \exp(\beta_2 z^0) + C_5 \exp(\gamma_1 z^0) + C_6 \exp(\gamma_2 z^0) + C_7 \exp(\lambda_1 z^0) + C_8 \exp(\lambda_2 z^0), \quad (44)$$

$$T^0 = C_1 \chi_1 \exp(\alpha_1 z^0) + C_2 \chi_2 \exp(\alpha_2 z^0), \quad (45)$$

$$U^0 = C_3 \chi_3 \exp(\beta_1 z^0) + C_4 \chi_4 \exp(\beta_2 z^0), \quad (46)$$

where

$$\alpha_1, \alpha_2 = \tfrac{1}{2}[-\phi_\infty^0 \pm (\phi_\infty^{02} + 4k^{02})^{\frac{1}{2}}], \quad (47)$$

$$\beta_1, \beta_2 = \frac{1}{2}\left\{-\frac{\phi_\infty^0}{Pr} \pm \left[\left(\frac{\phi_\infty^0}{Pr}\right)^2 + 4\left(k^{02} + \frac{2}{Pr^{\frac{2}{3}}}\right)\right]^{\frac{1}{2}}\right\}, \quad (48)$$

$$\gamma_1, \gamma_2 = \pm k^0, \quad (49)$$

$$\lambda_1, \lambda_2 = \frac{1}{2}\left\{-\frac{\phi_\infty^0}{Pr} \pm \left[\left(\frac{\phi_\infty^0}{Pr}\right)^2 + 4\left(k^{02} - \frac{1}{Pr^{\frac{2}{3}}}\right)\right]^{\frac{1}{2}}\right\}, \quad (50)$$

$$\chi_1 = \frac{\alpha_1^4 + \frac{\phi_\infty^0}{Pr}\alpha_1^3 + \left(\frac{1}{Pr^{\frac{2}{3}}} - 2k^{02}\right)\alpha_1^2 - \frac{\phi_\infty^0}{Pr}k^{02}\alpha_1 + k^{04} - \frac{k^{02}}{Pr^{\frac{2}{3}}}}{k^{02}Ra^0}, \quad (51)$$

$$\chi_2 = \frac{\alpha_2^4 + \frac{\phi_\infty^0}{Pr}\alpha_2^3 + \left(\frac{1}{Pr^{\frac{2}{3}}} - 2k^{02}\right)\alpha_2^2 - \frac{\phi_\infty^0}{Pr}k^{02}\alpha_2 + k^{04} - \frac{k^{02}}{Pr^{\frac{2}{3}}}}{k^{02}Ra^0}, \quad (52)$$

$$\chi_3 = -\frac{\beta_1^4 + \frac{\phi_\infty^0}{Pr}\beta_1^3 + \left(\frac{1}{Pr^{\frac{2}{3}}} - 2k^{02}\right)\beta_1^2 - \frac{\phi_\infty^0}{Pr}k^{02}\beta_1 + k^{04} - \frac{k^{02}}{Pr^{\frac{2}{3}}}}{\beta_1^3 + \frac{\phi_\infty^0}{Pr}\beta_1^2 + \left(\frac{1}{Pr^{\frac{2}{3}}} - k^{02}\right)\beta_1}, \quad (53)$$

$$\chi_4 = -\frac{\beta_2^4 + \frac{\phi_\infty^0}{Pr}\beta_2^3 + \left(\frac{1}{Pr^{\frac{2}{3}}} - 2k^{02}\right)\beta_2^2 - \frac{\phi_\infty^0}{Pr}k^{02}\beta_2 + k^{04} - \frac{k^{02}}{Pr^{\frac{2}{3}}}}{\beta_2^3 + \frac{\phi_\beta^0}{Pr}\beta_2^2 + \left(\frac{1}{Pr^{\frac{2}{3}}} - k^{02}\right)\beta_2}. \quad (54)$$

It should be pointed out that, although both λ_1 and λ_2 are negative when k^0 is less than $Pr^{-\frac{1}{3}}$, λ_1 does not represent a true decaying solution since it will approach zero as ϕ_∞ increases.

In order for the functions to remain finite, the constants C_1, C_3, C_5 and C_7 in front of these four growing solutions must be equal to zero. Since χ_2 and χ_4 are slowly varying functions of α_2, β_2, k^0, Pr and ϕ_∞^0, the decay rates of T^0 and U^0 are proportional to $\exp(\alpha_2 z^0)$ and $\exp(\beta_2 z^0)$ respectively. The decay rate of W^0 is determined by the slowest-decaying mode among $\exp(\alpha_2 z^0)$, $\exp(\beta_2 z^0)$, $\exp(\gamma_2 z^0)$ and $\exp(\lambda_2 z^0)$, and so is the decay behaviour of V^0.

ϕ^0 is a monotonically increasing function of z^0. It varies as z^{02} for Pr approaching infinity, and as z^0 for Pr around unity at the edge of the thermal boundary layer. The wavenumbers k^0 near the critical point for all the cases studied here are of the order of unity, as will be shown later. Thus the temperature disturbance T^0 near the critical point should decay approximately at the rate of $\exp(-\phi^0 z^0)$ beyond the thermal boundary layer. The decay rate of U^0 is also proportional to $\exp(-\phi^0 z^0)$ at

small Pr. As Pr increases, the decay rate of U^0 will shift to exp $(-k^0 z^0)$, and the height of propagation of the velocity disturbances in the streamwise direction depends on the wavelength at large Pr.

In addition to the two decaying modes discussed above, W^0 (as does V^0) has two more decaying modes, exp $(\gamma_2 z^0)$ and exp $(\lambda_2 z^0)$. The former is equal to exp $(-k^0 z^0)$. The latter exhibits similar decay behaviour to that of U^0. Thus we conclude the decay rate of W^0 is determined by the slowest-decaying mode, which is proportional to exp $(-k^0 z^0)$ around the critical point.

The above results clearly show that for $z^0 \gg 1/k^0$, the disturbance functions decay at rates considerably faster than the rate of change of the coefficients of (38)–(40). The assumption of constant coefficients, which amounts to the lowest-order WKB approximation, is hence justified.

5. The limiting case for Prandtl number approaching infinity

At very large Pr, the thermal boundary layer is much thinner than the viscous boundary layer. However, since the reference lengthscale used in (32)–(40) is proportional to the thickness of the thermal boundary layer, the results should converge asymptotically to a finite limit as Pr increases. For the limiting case of infinite Prandtl number, the base flow can be written explicitly as

$$\phi^0(z^0) = 0.5\,\phi^{0\prime\prime}(0)\,z^{02} = 0.616294\,z^{02} \quad \text{for} \quad Pr \to \infty, \tag{55}$$

$$\theta^0(z^0) = 1 - \frac{\displaystyle\int_0^{z^0} \exp\left(\int_0^{\zeta} -\phi^0\,\mathrm{d}\zeta\right)\mathrm{d}\zeta}{\displaystyle\int_0^{\infty} \exp\left(\int_0^{\zeta} -\phi^0\,\mathrm{d}\zeta\right)\mathrm{d}\zeta} \quad \text{for} \quad Pr \to \infty, \tag{56}$$

and the perturbation equations reduce to a sixth-order eigenvalue problem

$$W^{0\prime\prime\prime\prime} - 2k^{02}W^{0\prime\prime} + k^{04}W^0 - k^{02}Ra^0 T^0 = 0 \quad \text{for} \quad Pr \to \infty, \tag{57}$$

$$T^{0\prime\prime} + \phi^0 T^{0\prime} - k^{02}T^0 - \phi^{0\prime} W^0 = 0 \quad \text{for} \quad Pr \to \infty, \tag{58}$$

with boundary conditions

$$W^0 = W^{0\prime} = T^0 = 0 \quad (z^0 = 0, \infty), \tag{59}$$

This is a sixth-order eigenvalue problem because U^0 is equal to zero. The decay behaviour of the disturbances at the edge of the thermal boundary layer can be obtained in a manner similar to that described in §4. The approximate solutions outside the thermal boundary layer are

$$T^0 = C_2 \chi_6 \exp(\alpha_2 z^0), \tag{60}$$

$$W^0 = C_2 \exp(\alpha_2 z^0) + C_4 \exp(-k^0 z^0) + C_6\, z^0 \exp(-k^0 z^0), \tag{61}$$

where

$$\chi_6 = \frac{\alpha_2^4 - 2\alpha_2^2 k^{02} + k^{04}}{k^{02} Ra^0}. \tag{62}$$

Again, the temperature disturbance decays at the rate of exp $(-\phi^0_\infty z^0)$, and the velocity disturbances in the transverse and vertical directions decay at the rate of exp $(-k^0 z^0)$.

Because this sixth-order system is significantly simpler than the eighth-order system for finite Prandtl numbers, especially with respect to the asymptotic

behaviour at large z^0, the solution for this sixth-order system has been obtained and used as basis of comparison for the finite-Prandtl-number results.

6. Method of solution

The governing equations for the velocity and temperature perturbations contain two functions ϕ and θ, which represent the base-flow velocity and temperature distribution. These functions cannot be expressed analytically and must be determined either from tabulations, or, more conveniently and accurately, computed as needed, as is done here. Accordingly, a numerical solution method was used.

The method adopted was to employ the shooting method for a finite domain and then to seek the asymptotic value of the eigenvalue as the upper limit of the domain approaches infinity. The details of the implementation of the calculation are discussed as follows.

In brief, for a given Pr and k^0, trial values for the eigenvalue Ra^0 and for three boundary conditions, $U^{0\prime}(0)$, $W^{0\prime\prime\prime}(0)$ and $T^{0\prime}(0)$, were assigned. In addition, since the equations and the boundary conditions are homogeneous, the boundary condition $W^{0\prime\prime}(0)$ was assigned arbitrarily. These, together with the four known boundary conditions at $z^0 = 0$, as given in (41), permit a trial solution to be obtained as an initial value problem employing a fourth-order Runge–Kutta integration. At a sufficiently high value of $z^0 = z_f^0$, the quantities $U^0(z^0)$, $W'(z^0)$, $W^0(z^0)$, and $T(z^0)$ were evaluated. If the trial solutions were correct (meaning if the trial values Ra^0 and $U^{0\prime}(0)$, $T^{0\prime}(0)$, $W^{0\prime\prime\prime}(0)$ were correct), $U^0(z_f^0)$, $W^0(z_f^0)$, $W^{0\prime}(z_f^0)$, and $T^0(z_f^0)$ should vanish. If the latter four quantities did not vanish, a set of four new trial values were determined according to standard Newton–Raphson scheme.

The Newton–Raphson iteration scheme converges rapidly, but has a small circle of convergence. In order to ensure that good trial values are used, the computations proceeded according to a systematic extrapolation scheme. At first, a calculation was performed for a finite layer that was sufficiently thin relative to the intrinsic boundary-layer thickness so that the problem approached that of the classical Rayleigh–Bénard problem. Solutions for the latter were then used to obtain the four trial values. After the convergence of the iteration, the computed layer depth was systematically increased until a sufficiently large value of z_f^0 was reached. To determine the asymptotic value of the critical Rayleigh number Ra^0 for $z_f^0 \to \infty$, z_f^0 was increased by a fixed increment Δz_f^0 systematically,

$$z_{f,i+1}^0 = z_{f,i}^0 + \Delta z_f^0;$$

the change of Ra_i^0 is plotted against $z_{f,i}^0$ as shown in figure 2. The vertical coordinate in figure 2 is the quantity $(Ra_n^0 - Ra_{n+1}^0)/(Ra_n^0\,\Delta z_f^0)$. It is seen that the plot approximates a straight line, indicating that Ra_i^0 is a decreasing geometrical sequence. Accordingly, the asymptotic value Ra^0 can be computed by the formula

$$\begin{aligned} Ra^0 &= Ra_n^0 + \sum_{j=1}^{\infty} (Ra_{n+j}^0 - Ra_{n+j-1}^0) \\ &\approx Ra_n^0 + \sum_{j=1}^{\infty} (Ra_n^0 - Ra_{n-1}^0)\, r^j \\ &\approx Ra_n^0 + \frac{r(Ra_n^0 - Ra_{n-1}^0)}{1-r}, \end{aligned}$$

where Ra_n^0 denotes the value of the eigenvalue for the largest z_f^0 computed. The ratio r is determined from the slope of the plot in figure 2.

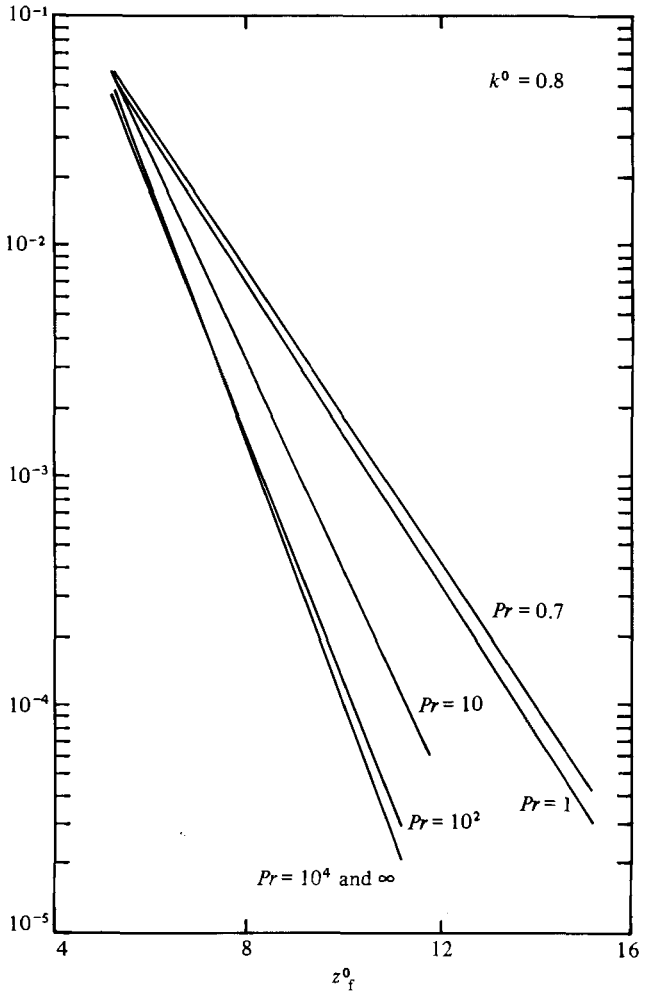

FIGURE 2. Method for determining the asymptotic solution (see text for discussion).

Typically, the computing depth employed was about 10–15 times the thermal scale (i.e. $z_f^0 = 10$–15), with 200–400 z-increments for wave-numbers around the critical wavenumber. Larger computing depth was employed for smaller-wavenumber cases. The integration arithmetic was a fourth-order Runge–Kutta method.

The obtained results have been compared with the results calculated by a matching method developed by Nachtsheim (1963) in his study of the thermal instability of natural-convection boundary layers. In this matching method, the results of the inner numerical shooting were forced to match the outer analytical solutions (described in §5) at a finite depth. The result of this comparison for $Pr = 1$, $k^0 = 0.8$, is shown in figure 3. The dashed line in this figure represents the calculated Ra^0 for different computing depths z_f^0, while the solid line represents the Ra^0 obtained from the matching method at different matching distances. The matching method shows a faster convergence; however, the outer boundary conditions for the numerical shooting in the matching method are more complicated than that encountered in the extrapolation method. Consequently, there was little saving in computer time and considerable increase in program complexity. Since the two methods provide

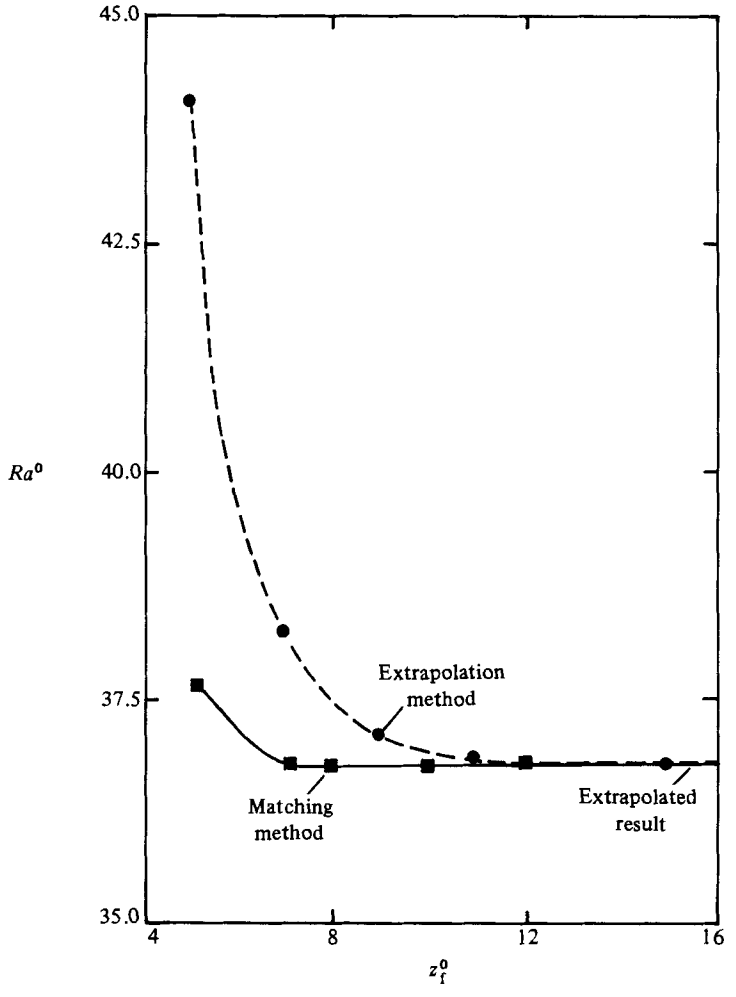

FIGURE 3. Comparison between the extrapolation method and the matching method for $Pr = 1$, $k^0 = 0.8$.

comparable accuracy, the extrapolation scheme was used for most of the computations.

7. Results and discussion

The calculated critical conditions and neutral stability curves for various Prandtl numbers are shown in table 1 and figures 4 and 5. It is seen from figure 4 that the critical wavenumber based on the viscous scale increases with increasing Pr, reflecting the gradual decrease in the thickness of the thermal boundary layer with increasing Pr.

Although the thermal scale length $(\nu/a)^{\frac{1}{2}}$ $(Pr^{-\frac{1}{2}})$ employed in §3 was derived from large-Prandtl-number considerations, it is interesting to note that it is also a very convenient lengthscale to use for moderate-Prandtl-number results. This is shown in figure 5, where the critical Rayleigh number is plotted against k^0, the dimensionless wavenumber based on the thermal scale. Note that the minimum wavenumber $k^0_{\min}$,

	$Pr = 0.7$	1	3	10	100	10^4	∞
z_∞^0	15.16	15.16	15.16	13.16	12.16	12.16	12.16
No. of steps N	200	200	200	300	300	400	400
k_c^0	0.783712	0.772323	0.743304	0.747269	0.795594	0.826650	0.833977
Ra_c^0	36.7286	36.7159	40.0142	46.3339	55.2188	60.7545	62.1801
Extrapolated k_c^0	0.7822	0.7710	0.7424	0.7468	0.7954	0.8266	0.8339
Extrapolated Ra_c^0	36.711	36.700	40.005	46.329	55.217	60.754	62.179

TABLE 1. Numerical data for the computation and results

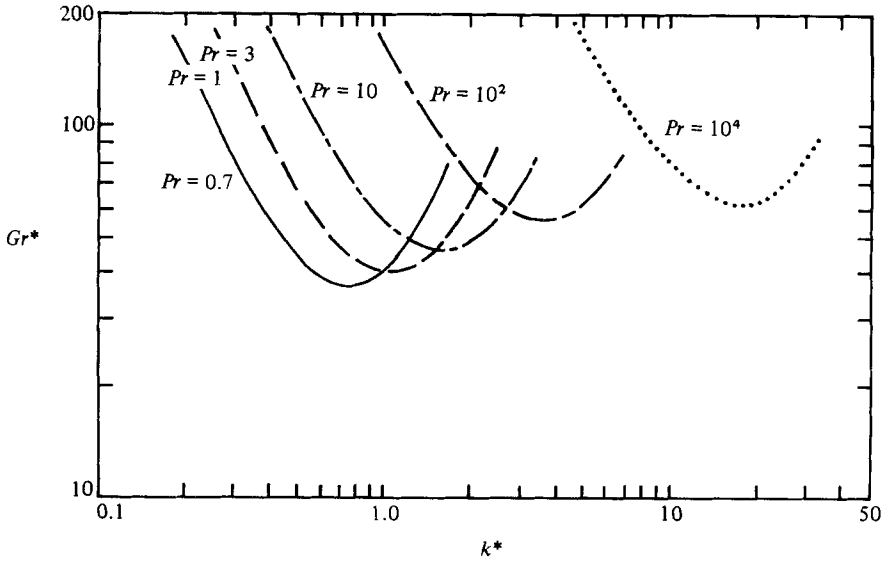

FIGURE 4. The critical Grashof number against the wavenumber k^*, both based on the viscous scale length.

depends only weakly on Pr, and the familiar fingerprint-like neutral stability curves are obtained. The reason for this, of course, is that the thermal-instability problem is essentially dependent on the thermal boundary-layer thickness and only weakly on the velocity distribution of the boundary layer. Since the thermal boundary layer thickness is essentially proportional to $Pr^{-\frac{1}{3}}$ for $1 < Pr < \infty$, the $Pr^{-\frac{1}{3}}$ dependence in the definition of the thermal scale length accounts approximately for the Prandtl-number dependence of the wavenumber.

The eigenfunctions W^0, V^0, U^0 and T^0 are shown in figures 6–8. Again, it is seen that the use of the stretched variable z^0 tends to clarify the Prandtl-number scaling relationship. Note, however, that there should not be too much significance attached to the magnitudes of W^0, V^0, U^0 and T^0 since the system of equations is homogeneous and the amplitude is essentially arbitrary. The magnitudes of U^0 and V^0 are relative to that of W^0.

From figures 7 and 8 the influence of the wavenumber on the disturbances propagation in the vertical direction may be observed clearly. As was shown analytically in §4, the decay rate of T^0 is always proportional to $\exp(-\phi^0 z^0)$ beyond the thermal boundary layer. The temperature disturbance is essentially confined within the thermal boundary layer since ϕ^0 increases with z^0, and thus $\exp(-\phi^0 z^0)$ represents a very fast decaying solution with respect to z^0. Also, it can be seen from figures 6 and 7 that the decay rate of T^0 for $Pr = 10^4$ is greater than that for $Pr = 1$, since at the edge of the thermal boundary layer, ϕ^0 is proportional to z^{02} at large Pr, but only proportional to z^0 at small Pr. The streamwise velocity disturbance shows the same decay behaviour at small Pr, as discussed above. At $Pr = 10^4$, the decay rate of U^0 should be proportional to $\exp(-k^0 z^0)$. However, the ratio of the magnitude of U^0 to that of W^0 decreases as $Pr^{-\frac{1}{3}}$. The shift in decay rate of U^0 at large Pr is difficult to observe clearly. Different values of k^0 will change only the decay rate of W^0 and V^0, and hence the dimensions of the convection cells. The smaller the wavenumber, the taller and wider the convection cells should be.

It is interesting to relate the present results to the results of Rayleigh–Bénard

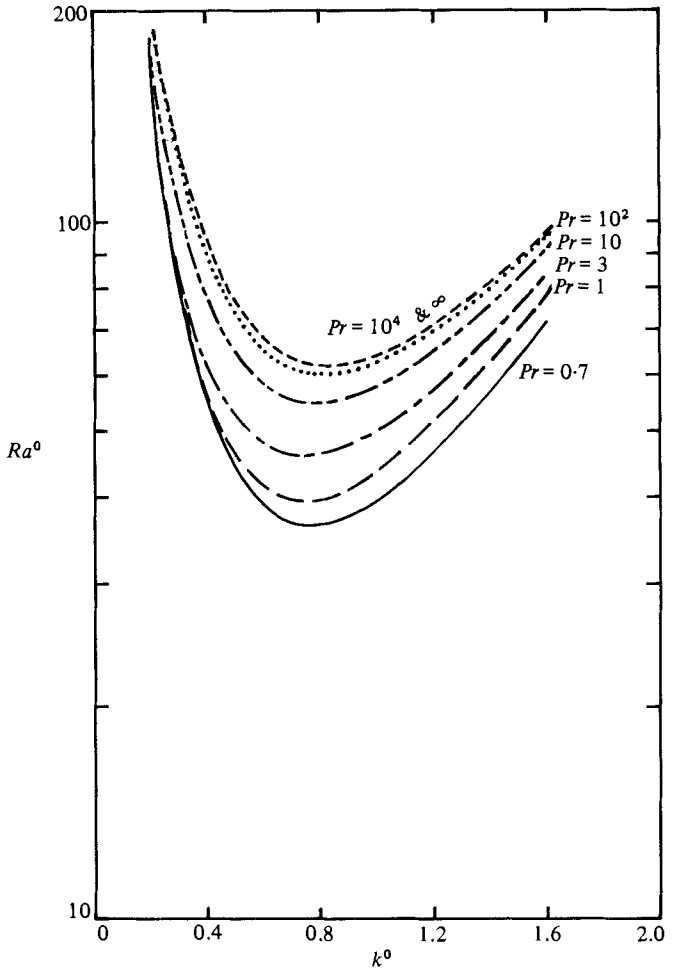

FIGURE 5. The critical Rayleigh number versus the wavenumber k^0, both based on the thermal scale length.

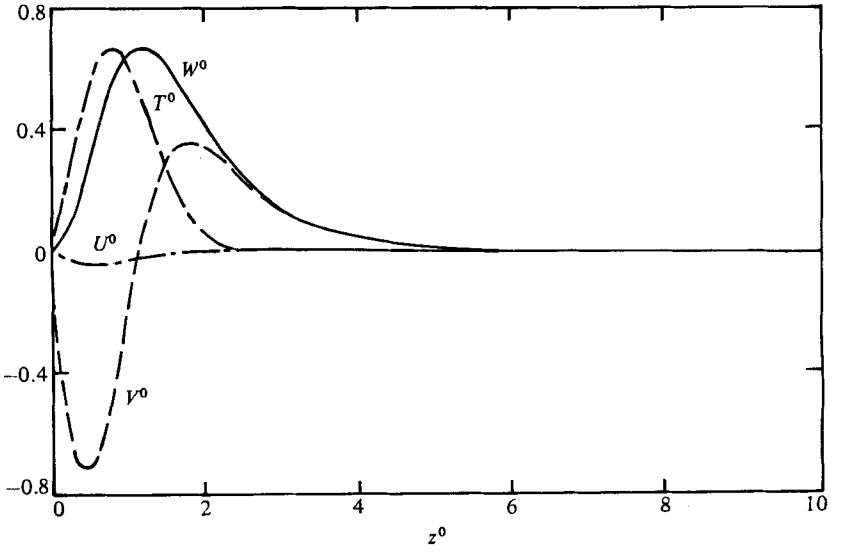

FIGURE 6. The eigenfunctions for $Pr = 1$; $k^0 = 0.772323$.

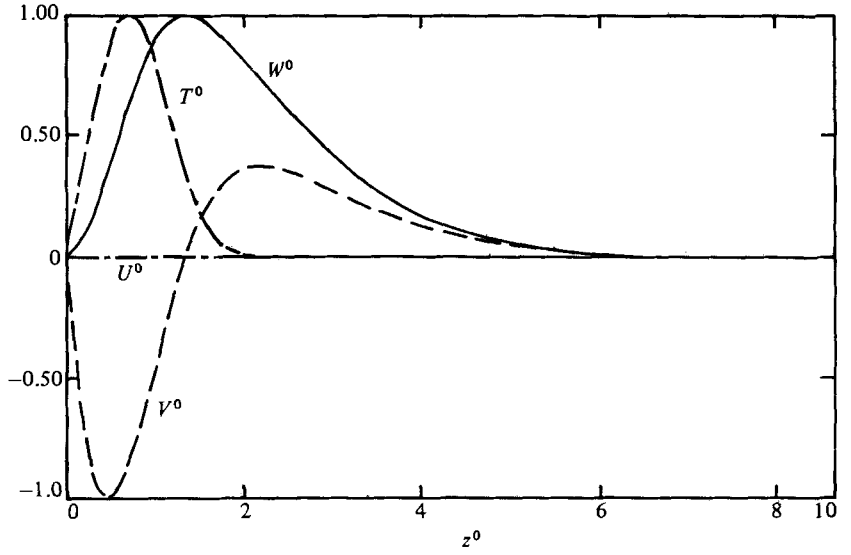

FIGURE 7. The eigenfunctions for $Pr = 10^4$; $k^0 = 0.826650$.

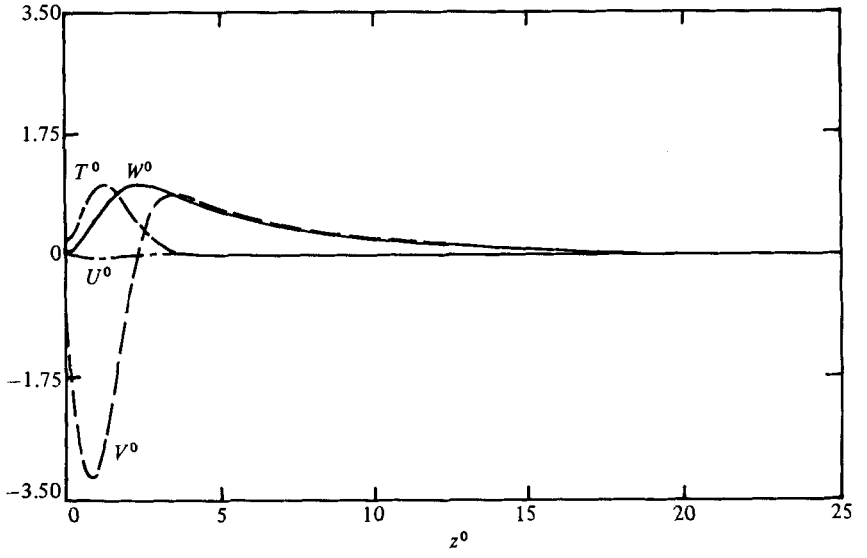

FIGURE 8. The eigenfunctions for $Pr = 1$; $k^0 = 0.2$.

instability without flow. Examination of the eigenfunctions presented in figures 6, 7 and 8 suggest that T^0 and W^0 are at their maximums between $z^0 = 1$–2. Thus, semiquantitatively, the disturbances in the fluid within 1–2 thermal scale lengths somewhat resemble those in the lower half of the classical Rayleigh–Bénard problem. Accordingly, one would expect that the critical Rayleigh number should be of the order of $\frac{1}{8}(= (\frac{1}{2})^3)$ of that of the Rayleigh–Bénard problem, or about 27–214. Because of the third-power dependence of the Rayleigh number on the length-scale, this type of estimate cannot be expected to be quantitatively accurate. The fact that our computed Rayleigh-number range of 37–62 was not far from this estimate attests to

the close relationship of the thermal instability of the boundary layers to that of the basic Rayleigh–Bénard problem.

Although there are a number of published experimental studies with information on the impingement region of thermal plumes, including those with clearly two-dimensional geometry, there is not enough information in the papers to facilitate a comparison with the present analysis. It is hoped that this study will stimulate interest in this area.

One interesting interpretation of the results can be made as follows. Since the lengthscale in the definition of Ra^0 is essentially a measure of the thermal boundary-layer thickness for high and moderate Prandtl numbers, the existence of the critical Rayleigh number suggests that there exists a maximum thermal boundary-layer thickness above which the boundary layer is thermally unstable. This, in turn, implies that there exists a minimum heat transfer coefficient below which the boundary layer is unstable. Making use of the fact that $\theta^{0\prime}(0) = -0.643$ for $Pr \gg 1$, it can be shown that the minimum heat transfer coefficient $h_{\min}$ is given by the expression

$$h_{\min} = 0.164 \left[\frac{g\beta\Delta t}{\alpha\nu}\right]^{\frac{1}{3}} \kappa,$$

where κ is the thermal conductivity.

Experimental verification and further theoretical exploration of this phenomenon would clearly be in order.

REFERENCES

Chandra, K. 1938 *Proc. R. Soc. Lond.* **A164**, 231.

Chen, M. M. 1971 *Bull Am. Phys. Soc.* **16**, 1310.

Chen, T. S. & Mucoglu, A. 1979 *Int. J. Heat Mass Transfer* **22**, 185.

Cheng, K. C. & Wu, R. S. 1976 *Trans ASME C: J. Heat Transfer* **98**, 565.

Ingersoll, A. P. 1966 *Phys. Fluids* **9**, 682.

Lloyd, J. R. & Sparrow, E. M. 1970 *J. Fluid Mech.* **42**, 465.

Nachtsheim, P. R. 1963 *NASA TN* D-2089.

Sparrow, E. M. & Husar, R. B. 1969 *J. Fluid Mech.* **37**, 251.